



# Angular momentum distributions of Rydberg state electrons of Be-like sulfur produced through foil penetration

M. Imai <sup>a,\*</sup>, M. Sataka <sup>b</sup>, S. Kitazawa <sup>b</sup>, K. Komaki <sup>c</sup>, K. Kawatsura <sup>d</sup>,  
H. Shibata <sup>e</sup>, H. Tawara <sup>f,g</sup>, T. Azuma <sup>h</sup>, Y. Kanai <sup>i</sup>, Y. Yamazaki <sup>c,i</sup>

<sup>a</sup> Department of Nuclear Engineering, Kyoto University, Sakyo, Kyoto 606-8501, Japan

<sup>b</sup> Department of Materials Science, Japan Atomic Energy Research Institute, Tokai, Ibaraki 319-1195, Japan

<sup>c</sup> Institute of Physics, Graduate School of Arts and Sciences, University of Tokyo, Meguro, Tokyo 153-8902, Japan

<sup>d</sup> Department of Chemistry and Materials Technology, Kyoto Institute of Technology, Kyoto 606-8585, Japan

<sup>e</sup> Research Center for Nuclear Science and Technology, University of Tokyo, Tokai, Ibaraki 319-1188, Japan

<sup>f</sup> Department of Physics, Kansas State University, Manhattan, KS 66506-2601, USA

<sup>g</sup> Atomic Physics Division, National Institute of Standards and Technology, Gaithersburg, MD 20899-8421, USA

<sup>h</sup> Department of Physics, Tokyo Metropolitan University, Hachioji, Tokyo 192-0397, Japan

<sup>i</sup> Atomic Physics Laboratory, The Institute of Physical and Chemical Research, Wako, Saitama 351-0198, Japan

## Abstract

Spectra for Coster–Kronig (C–K) transition  $1s^2 2p(^2P_{3/2})9l \rightarrow 1s^2 2s(^2S_{1/2})\epsilon l'$  of Be-like  $S^{12+}$  ions produced following penetration of 2.5 MeV/u  $S^{q+}$  ions ( $q = 7, 10, 12, 13$ ) through C-foil targets of various thickness (1–6.9  $\mu\text{g}/\text{cm}^2$ ) have been probed using zero-degree electron spectroscopy. It has been found that in collisions for  $S^{q+}$  ( $q = 7, 10$ ) ion incidence, in which the C–K electrons originate from the projectile bound electrons, a fraction of the angular momentum  $l = 1$  of the Rydberg state decreases, and fractions of higher ( $l \geq 2$ ) angular momenta increase, while the total intensity of the C–K electrons grows, as target foil thickness increases. The electron spectra for  $S^{q+}$  ( $q = 13$ ) incident ions, in which the autoionizing Be-like state is preferably formed by electron capture from the target continuum upon or near the exiting surface, do not change in  $l$ -distribution or intensity. The shift to higher  $l$  comes from the multiple collisions of electron with the target, in traveling at the same speed under the strong Coulomb potential of the projectile. The observed dependence of the  $l$ -distribution and the intensity of the Rydberg state on projectile initial charge and target thickness indicates the importance of transport phenomena for both the  $S^{13+}$  core and the projectile-entrained electrons inside solid. © 2002 Elsevier Science B.V. All rights reserved.

PACS: 34.50.Fa; 34.60.+z

Keywords: Rydberg state; Excitation; Ionization; Charge transfer; Non-equilibrium mean charge

## 1. Introduction

It already has been established through photon spectroscopy [1,2] as well as electron spectroscopy [3,4] that the Rydberg states formed via collisions in foil targets have higher angular momenta,

\* Corresponding author. Fax: +81-75-753-5845.

E-mail address: imai@nucleng.kyoto-u.ac.jp (M. Imai).

compared with those formed in gas-phase collisions. In ion-solid collision, the Rydberg states are not expected to be formed through direct capture of “target” electron at the last layers of solid, nor survive target penetration because the orbital radius of Rydberg electron is far larger than the lattice spacings in solids. Instead, the Rydberg states are formed by re-capturing the electron, which was released from projectile bound state at an earlier stage of penetration and moved inside the solid at the projectile velocity, caused by a sudden switch of potential (from screened to normal Coulomb) at the exit surface [5]. The higher angular momenta in foil targets than in gas targets suggest that the electron gets higher angular momentum via multiple collisions with atoms through foil-transportation under the strong influence of the projectile, as the electron should keep its angular momentum in the re-capture process. Burgdörfer and Bottcher [6] have developed a classical transport theory of near-threshold excitation of electrons inside solid (called entrained electrons), and succeeded in reproducing the experimental result quantitatively. Continuous investigations [7–9] have been made to understand the detailed mechanisms.

So far zero-degree electron spectroscopy [10,11] has proved to be one of the most powerful tools to study the Rydberg state ions consisting of the excited core ion and Rydberg electron, through observing the Coster–Kronig (C–K) electrons ejected at zero degrees with high resolution [3,12].

We have been studying the electron emission mechanisms from various ions with different energy passing through gas and solid targets with zero-degree electron spectroscopy [13–17]. We measured the C–K electrons from Be-like configuration  $1s^2 2p(^2P_{3/2}^\circ)nl$  or  $1s^2 2p(^2P_{1/2}^\circ)nl \rightarrow 1s^2 2s(^2S_{1/2})\epsilon l'$  created by passage of 64 MeV (2.0 MeV/u)  $S^{12+}$  ions through He or C-foil targets, and have observed significant differences of the  $l$ -distribution for the gas and solid phase targets [4,18], and dependence of the product  $l$ -distribution on foil thickness and projectile charge state [19]. According to the picture of the Rydberg state formation after foil penetration, it is important whether the initial ion brings more or less than four electrons to form

the Be-like Rydberg state as well as the charge state distribution (or the mean charge state) of the projectile after “or through” penetration. In the present work, we describe our systematic measurements of C–K electron spectra from 2.5 MeV/u  $S^{7+}$ ,  $S^{10+}$ ,  $S^{12+}$  and  $S^{13+}$  ions incident on carbon-foil targets with various thicknesses of 1–6.9  $\mu\text{g}/\text{cm}^2$ . These targets meet our destination as they are far thicker than the escape-depth of the captured electron, which is assumed to be  $\sim 10 \text{ \AA}$ , corresponding to a foil thickness of  $\sim 0.2 \mu\text{g}/\text{cm}^2$ .

## 2. Experiments

The present experiments were performed at the tandem accelerator facility at the Japan Atomic Energy Research Institute (JAERI), Tokai. As a detailed description of the experimental apparatus has been presented previously [4,13–19], only some major parameters are given here. A beam of 80 MeV (2.5 MeV/u)  $S^{7+}$  ions was obtained from the tandem accelerator. The primary  $S^{7+}$  or post-stripped  $S^{q+}$  ( $q = 10$ –13) ions were guided onto the target foils which were kept in a collision chamber at a base pressure of  $10^{-8}$  Torr and were finally collected with a Faraday cup. Electrons emitted from the projectile ions after passage through self-supported C-foil targets of 1.1–6.9  $\mu\text{g}/\text{cm}^2$  were energy analyzed with a tandem electrostatic analyzer located at zero degrees with respect to the ion beam direction. The electron-pass energy for the second analyzer was set at 50 eV to improve the resolution and also to keep its transmission constant. Electron spectra in the laboratory frame were obtained by scanning the retarding potential between the first and the second analyzers in 1 or 0.5 V steps for a fixed integrated ion beam current at the Faraday cup. The observed electron spectra were dominated by the so-called cusp peak at around 1.39 keV and a series of C–K electron peaks were superposed on both wings of the cusp (see Fig. 1(a)). Two spectra for the backward and forward ejected electrons, corresponding to the low and high energy wings of the cusp, respectively, were obtained by converting data points into the projectile rest frame from the laboratory frame. This conversion resulted in the energy

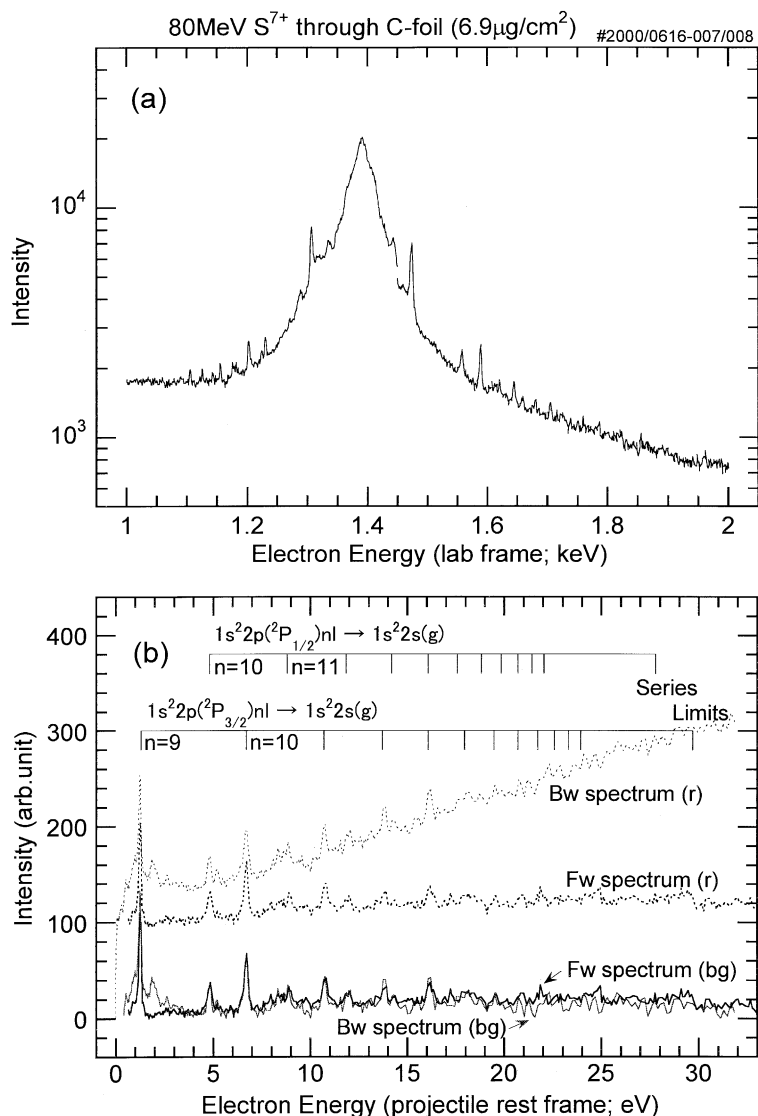


Fig. 1. (a) Electron energy spectrum in the laboratory frame for 80 MeV  $S^{7+}$  ions passing through  $6.9 \mu\text{g}/\text{cm}^2$  carbon-foil measured at zero degrees. (b) Electron energy spectra transformed into the projectile rest frame. The thin dotted curves correspond to the energy spectra for the forward (denoted as Fw) and backward (denoted as Bw) scattering, and the solid curves are background-subtracted spectra. The repetitive peaks are assigned to C–K transitions, whose configurations and energies are indicated in the figure, using formula (1) in text.

resolution of 0.01–0.05 eV at the electron energy region of our interest ( $\sim 2$  eV). The spectrum from the high energy wing, which is denoted as “Fw spectrum (r)” in Fig. 1(b), has a constant background which comes from a part of the cusp electrons, meanwhile the low energy wing spectrum, which is denoted as “Bw spectrum (r)”, has

additional backgrounds coming from soft collisions (see the dotted curves in Fig. 1(b)). After subtracting these backgrounds, the spectra have practically the same energy and intensity distributions (see the solid curves in Fig. 1(b)), confirming the constant transmission of our electron analyzer system in the measured region.

### 3. Results and discussion

The repetitive peaks in Fig. 1(b) are assigned to the C–K transitions  $1s^2 2p(^2P_{3/2}^\circ)nl$  ( $n \geq 9$ )  $\rightarrow$   $1s^2 2s\ell'$  or  $1s^2 2p(^2P_{1/2}^\circ)nl$  ( $n \geq 10$ )  $\rightarrow$   $1s^2 2s\ell'$  of Be-like  $S^{12+}$  ions, using the formula

$$E_{C-K} = \Delta E - Q^2 Ry/2n^2, \quad (1)$$

where  $E_{C-K}$  is the C–K electron energy,  $\Delta E$  is the energy difference between the initial and the final states of the core ion configurations, taken from the compiled transition energy tables [20,21],  $Q$  is the effective charge of the  $S^{13+} 1s^2 2p(^2P)$  core ion (assumed to be +13 for this case), and  $Ry/2$  is the Rydberg energy (13.6 eV). Hereafter, we focus on the details of the most intense peak of the  $1s^2 2p(^2P_{3/2}^\circ)9l \rightarrow 1s^2 2s\ell'$  transition. Electron energy spectra from the C–K transition formed by 80 MeV  $S^{7+}$ ,  $S^{10+}$ ,  $S^{12+}$  and  $S^{13+}$  ions incident through C-foil targets of various thicknesses are shown in Fig. 2. In the figure, the observed electron spectra are normalized to the fixed number of the impinging ions using factors (mean charge for each collision system)/(equilibrium mean charge = 13.3 [22–24]), where the mean charges of S ions after foil passage were estimated from the variations of the Faraday cup current when switching the target foils in/out (Table 1). The vertical bars on top in the figure show the C–K electron energies calculated using the Z-expansion method (MZ code) [25] with state descriptions for  $1s^2 2p9l$  Rydberg configuration on the right hand. These calculated values are shifted by  $-0.2$  eV, as discussed in Ref. [25] to compensate the difference with experimental results for  $n \leq 19$ . Energies for  $l \geq 4$  states are not available from the MZ code in Ref. [25]. The length of the vertical bar indicates the autoionization rate associated with the transition, calculated with the multi-configuration Hartree–Fock method (Cowan code) [25]. We have carefully checked that no Rydberg state of  $S^{q+}$  ( $7 \leq q \leq 13$ ) ions, other than the  $1s^2 2p(^2P_{3/2}^\circ)9l$  states of  $S^{12+}$ , can give rise to peaks in the present energy range, based upon the formula (1).

Fig. 2 demonstrates that the intensity of the prominent peak at around 1.25 eV increases dramatically for incident  $S^{7+}$  and  $S^{10+}$  ions as the target thickness increases. For  $S^{12+}$  collision, a

small increase is found which saturates at target thickness of  $2.0 \mu\text{g}/\text{cm}^2$ , and the intensity and shape of the peak do not depend on target thickness for  $S^{13+}$ . These behaviors can be understood generally by the number of  $S^{13+}$  core ions and of entrained electrons, released from the projectile, inside the target. Considering the mean charges for each foil, and thus the number of electrons expected to be released, in Table 1, the nearly proportional increase of the peak intensity with foil thickness for the  $S^{7+}$  and  $S^{10+}$  ions incidence is characterized mainly by the increase in the  $S^{13+}$  core production. The small increase for the  $S^{12+}$  ions is characterized by both  $S^{13+}$  core ions and entrained electrons. The dependence of total electron intensity on the projectile initial charge state at fixed target thickness can be understood in the same manner. The increase of the peak intensity due to the increase of initial charge from 7+ to 10+ is characterized by the increasing number of the core ions, and the decrease for 12+ and 13+ initial charge states for  $2.0$ – $6.9 \mu\text{g}/\text{cm}^2$  targets is described by a decrease in electrons released from projectile. We point out that not only the number of entrained electrons but charge evolution of the projectile inside solid should be included for the practical understanding of the peak intensity dependence on foil thickness and projectile initial charge.

Next, the shape of the peak and its change for each collision system is treated qualitatively. With a help of energy calculations using the MZ code, we consider the peak at around 1.25 eV to originate from  $1s^2 2p9l$  configurations, whose  $l$  is larger than or equal to 2. The shoulder at around 1.15 eV, which can be seen in most of the spectra, is likely to come from configurations with lower angular momentum ( $l = 1$ ), considering the large autoionization rate of  $1s^2 2p9p \ ^1S_0$  configuration. In the  $S^{7+}$  incidence, the shoulder appears for the  $2.0$  and  $6.9 \mu\text{g}/\text{cm}^2$  targets, and for the latter, the shoulder becomes relatively weak compared with the prominent peak at around 1.25 eV in spite of the increase of the shoulder intensity. The same tendency is found for  $S^{10+}$ , and a weak shoulder is seen only for the  $1.5$  and  $2.0 \mu\text{g}/\text{cm}^2$  targets in  $S^{12+}$  incidence. For  $S^{13+}$ , there is no dependence of either peak shape or intensity on target thickness. As

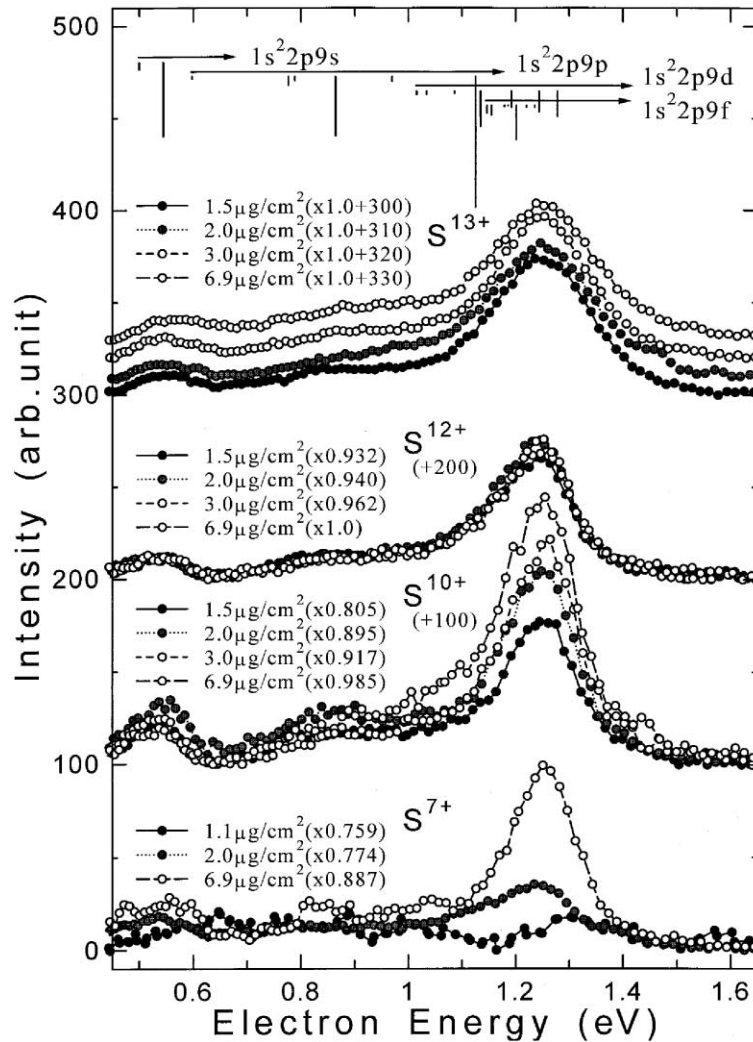


Fig. 2. Electron energy spectra from C-K transitions  $1s^2 2p(^2P_{3/2})9l \rightarrow 1s^2 2s\epsilon l'$  formed through 80 MeV  $S^{7+}$ ,  $S^{10+}$ ,  $S^{12+}$  and  $S^{13+}$  ions colliding with C-foil targets with various thickness. Each spectrum is normalized to the integrated number of the impinging particles (see text).

described previously, the autoionizing Rydberg electron is considered to have its origin in projectile bound electrons, which was released and traveled inside the foil undergoing multiple collisions, for  $S^{7+}$ ,  $S^{10+}$  and  $S^{12+}$  ions incidence. The appearance of the shoulder can be attributed to the  $l(=1)$ -population of the entrained electrons, and the decrease of the shoulder ratio is due to the shift to higher  $l$  values, reflecting multiple collisions of the entrained electrons with the target under the

strong influence of the projectile, as has been shown experimentally [3] and theoretically [6] for  $1s^2 2p5l \rightarrow 1s^2 2s\epsilon l'$  transition of 1.5 MeV  $C^{2+}$  ions. The importance of transport phenomena is demonstrated again by the longer survival of  $l = 1$  population for  $S^{7+}$  and  $S^{10+}$  ions incidence, where more projectile bound electrons are expected to be released during foil penetration, than for  $S^{12+}$ . For  $S^{13+}$ , however, the release of the projectile bound electron and formation of entrained electrons have

Table 1

The estimated mean charge for incident 80 MeV S<sup>q+</sup> ions after passing through thin carbon foils with various thickness, obtained by measuring the variation of the Faraday cup current with and without the carbon foil present

Foil thickness ( $\mu\text{g}/\text{cm}^2$ )	Projectile incident charge state			
	S <sup>7+</sup>	S <sup>10+</sup>	S <sup>12+</sup>	S <sup>13+</sup>
1.1	10.1	–	–	–
1.5	–	10.7	12.4	13.3
2.0	10.3	11.9	12.5	13.3
3.0	–	12.2	12.8	13.3
6.9	11.8	13.1	13.3	13.3

The (nominal) equilibrium charge is known to be 13.3 for 80 MeV S ions [22–24].

little possibility, and the autoionizing Rydberg state is formed by electron capture from target continuum upon or near the exiting surface, which agree our observation of no dependence of intensity and *l*-distribution on the target thickness.

### Acknowledgements

HT was supported (in part) by the Chemical Sciences, Geosciences, and Biosciences Division, Office of Basic Energy Science, US Department of Energy.

### References

- [1] J. Rothermal, H.-D. Betz, F. Bell, V. Zacek, Nucl. Instr. and Meth. 194 (1982) 341.
- [2] H.-D. Betz, J. Rothermal, D. Rösenthaller, F. Bell, R. Schuch, G. Nolte, Phys. Lett. A 91 (1982) 12.
- [3] Y. Yamazaki et al., Phys. Rev. Lett. 61 (1988) 2913.
- [4] K. Kawatsura et al., Nucl. Instr. and Meth. B 48 (1990) 103.
- [5] H.-D. Betz, D. Rösenthaller, J. Rothermal, Phys. Rev. Lett. 50 (1983) 34.
- [6] J. Burgdörfer, C. Bottcher, Phys. Rev. Lett. 61 (1988) 2917.
- [7] C.O. Reinhold, D.G. Arbó, J. Burgdörfer, B. Gervais, E. Lamour, D. Vernhet, J.P. Rozet, J. Phys. B 33 (2000) L111.
- [8] M. Beuve, B. Gervais, E. Lamour, J.P. Rozet, D. Vernhet, L.J. Dubé, Phys. Lett. A 274 (2000) 37.
- [9] D. Vernhet, J.P. Rozet, I. Bailly-Despiney, C. Stephan, A. Cassimi, J.P. Grandin, L.J. Dubé, J. Phys. B 31 (1998) 117.
- [10] N. Stolterfoht, Phys. Rep. 146 (1987) 315.
- [11] A. Itoh, T. Schneider, G. Schiwietz, Z. Roller, H. Platten, G. Nolte, D. Schneider, N. Stolterfoht, J. Phys. B 16 (1983) 3965.
- [12] Y. Yamazaki, Nucl. Instr. and Meth. B 96 (1995) 517.
- [13] M. Sataka et al., Phys. Rev. A 44 (1991) 7290.
- [14] K. Kawatsura et al., J. Electron Spectrosc. Relat. Phenom. 88–91 (1998) 83.
- [15] K. Kawatsura et al., Nucl. Instr. and Meth. B 53 (1991) 421.
- [16] M. Imai, M. Sataka, Y. Yamazaki, K. Komaki, K. Kawatsura, Y. Kanai, Phys. Scr. T73 (1997) 93.
- [17] K. Kawatsura et al., J. Electron Spectrosc. Relat. Phenom. 88–91 (1998) 87.
- [18] K. Kawatsura, M. Sataka, M. Imai, K. Komaki, Y. Yamazaki, K. Kuroki, Y. Kanai, S. Arai, N. Stolterfoht, Nucl. Instr. and Meth. B 124 (1997) 381.
- [19] M. Imai, M. Sataka, H. Naramoto, Y. Yamazaki, K. Komaki, K. Kawatsura, Y. Kanai, Nucl. Instr. and Meth. B 67 (1992) 142.
- [20] R.L. Kelly, J. Phys. Chem. Ref. Data 16 (Suppl. 1) (1987).
- [21] V. Kaufman, W.C. Martin, J. Phys. Chem. Ref. Data 22 (1993) 279.
- [22] U. Scharfer, C. Henrichs, J.D. Fox, P. von Brentano, L. Degener, J.C. Sens, A. Pape, Nucl. Instr. and Meth. 146 (1977) 573.
- [23] K. Shima, T. Mikumo, H. Tawara, At. Data Nucl. Data Tables 34 (1986) 357.
- [24] K. Shima, N. Kuno, M. Yamanouchi, H. Tawara, At. Data Nucl. Data Tables 51 (1992) 173.
- [25] I.Yu. Tolstikhina, H. Tawara, U.I. Safronova, M. Imai, M. Sataka, K. Kawatsura, K. Komaki, Y. Yamazaki, Phys. Scr. 54 (1996) 188.